IT ISSN 0391 - 9838

Bollettino del Comitato Glaciologico Italiano - ser. 3

GEOGRAFIA FISICA e DINAMICA QUATERNARIA

An international Journal published under the auspices of the
Rivista internazionale pubblicata sotto gli auspici di

Associazione Italiana di Geografia Fisica e Geomorfologia
and (e) Consiglio Nazionale delle Ricerche (CNR)

recognized by the (*riconosciuta da*)

International Association of Geomorphologists (IAG)

volume 41 (2)
2018

COMITATO GLACIOLOGICO ITALIANO - TORINO
2018

GEOGRAFIA FISICA E DINAMICA QUATERNARIA

A journal published by the Comitato Glaciologico Italiano, under the auspices of the Associazione Italiana di Geografia Fisica e Geomorfologia and the Consiglio Nazionale delle Ricerche of Italy. Founded in 1978, it is the continuation of the «Bollettino del Comitato Glaciologico Italiano». It publishes original papers, short communications, news and book reviews of Physical Geography, Glaciology, Geomorphology and Quaternary Geology. The journal furthermore publishes the annual reports on italian glaciers, the official transactions of the Comitato Glaciologico Italiano and the Newsletters of the Intemational Association of Geomorphologists. Special issues, named «Geografia Fisica e Dinamica Quaternaria - Supplementi», collecting papers on specific themes, proceedings of meetings or symposia, regional studies, are also published, starting from 1988. The language of the journal is English, but papers can be written in other main scientific languages.

Rivista edita dal Comitato Glaciologico Italiano, sotto gli auspici dell'Associazione Italiana di Geografia Fisica e Geomorfologia e del Consiglio Nazionale delle Ricerche. Fondata nel 1978, è la continuazione del «Bollettino del Comitato Glaciologico Italiano». La rivista pubblica memorie e note originali, recensioni, corrispondenze e notiziari di Geografia Fisica, Glaciologia, Geomorfologia e Geologia del Quaternario, oltre agli Atti ufficiali del C.G.I., le Newsletters della I.A.G. e le relazioni delle campagne glaciologiche annuali. Dal 1988 vengono pubblicati anche volumi tematici, che raccolgono lavori su argomenti specifici, atti di congressi e simposi, monografie regionali sotto la denominazione «Geografia Fisica e Dinamica Quaternaria - Supplementi». La lingua usata dalla rivista è l'Inglese, ma gli articoli possono essere scritti anche nelle altre principali lingue scientifiche.

Indexed/Abstracted in: Bibliography & Index of Geology (GeoRef); GeoArchive (Geosystem); GEOBASE (Elsevier); *Geographical Abstract*: *Physical Geography* (Elsevier); GeoRef; Geotitles (Geosystem); Hydrotitles and Hydrology Infobase (Geosystem); Referativnyi Zhurnal.
Geografia Fisica e Dinamica Quaternaria has been included in the Thomson ISI database beginning with volume 30 (1) 2007 and now appears in the Web of Science, including the Science Citation Index Expanded (SCIE), as well as the ISI Alerting Services.

HOME PAGE: http://gfdq.glaciologia.it/ - CONTACT: gfdq@dst.unipi.it

Printed with the financial support from (pubblicazione realizzata con il contributo finanziario di):

– Comitato Glaciologico Italiano
– Associazione Italiana di Geografia Fisica e Geomorfologia
– Ministero dell'Istruzione, Università e Ricerca
– Consiglio Nazionale delle Ricerche
– Club Alpino Italiano

Comitato Glaciologico Italiano
President (*Presidente*) M. Frezzotti

Geogr. Fis. Dinam. Quat.
41 (2018). 95-104, 12 figg., 1 tab.

DOI 10.4461/ GFDQ.2018.41.15

REZA ZAKERINEJAD [1*], ADEL OMRAN [2,3], VOLKER HOCHSCHILD [2] &
MICHAEL MAERKER [4]

ASSESSMENT OF GULLY EROSION IN RELATION TO LITHOLOGY IN THE SOUTHWESTERN ZAGROS MOUNTAINS, IRAN USING ASTER DATA, GIS AND STOCHASTIC MODELING

Abstract: *Assessment of gully erosion in relation to lithology in the southwestern Zagros Mountains, Iran using ASTER data, GIS and stochastic modeling.* (IT ISSN 0391-9839, 2018).

Soil erosion in arid areas is a major environmental threat. Gullies, as one of the most intensive soil erosion processes, are very common in the southwest of Iran. Lithology, vegetation density and climate change, as well as land use and land cover change are effective drivers of soil loss in general, and gully erosion in particular. The overall objective of this research is to assess the relation between, lithology and the spatial distribution of gullies in the Mazayjan basin. Data were collected by field survey, interpreting aerial photos and analyzing ASTER multispectral images. Modeling of spatial gully susceptibility was performed with a GIS-based statistical mechanics approach (Maxent). The analysis of ASTER bands ratios yields valuable results in terms of the mineral differentiation of the Zagros Mountain substrates and hence, can be utilized as a tool for lithological mapping. Additionally, the statistical mechanics approach used to assess the relation between existing gully locations and the combinations of lithologic predictor variables show that gullies have a high probability in areas showing substrates with high amounts of salt, gypsum and marl, especially in the plain areas. The model performance shows a very high accuracy both for train and test data. The spatial prediction highlights concentrated gully erosion in areas with aeolian sediments on top of alluvial substrates.

Key Words: Gully erosion, ASTER multispectral data, lithology, topographic indices.

INTRODUCTION

In southern and southwestern Iran, gully erosion is one of the most serious types of soil erosion causing land degradation in cultivated and range land areas (Wasson & *alii*, 2002; Masoudi & Zakerinejad, 2010; Shahrivar & *alii*, 2012; Zakerinejad & Maerker, 2014). The diversity and impact of various factors driving the formation and development of gully erosion are highly variable. Thus, the understanding of the most significant drivers of gully initiation is an important prerequisite to improve land use management and to prevent soil erosion. Gully erosion is the major land degradation process notably in arid and semi-arid areas (see Pickup, 1991; Pringle & *alii*, 2006).

Various researchers have studied the factors and mechanisms which affect gullying in many parts of the world with major emphasis on arid and semi-arid areas (Ghodosi, 2006; Kheir & *alii*, 2007; Samani & *alii*, 2010; Shahrivar & *alii*, 2012; Zakerinejad & Maerker, 2015). Areas with scarce vegetation and a high amount of silty soils are particularly affected. Most gullies occur in unconsolidated materials, including colluvium and alluvium, deeply weathered substrates (Ahmadi, 2007; Conoscenti & *alii*, 2008; Maerker & *alii*, 2008; Frankl & *alii*, 2012) or aeolian deposits such as loess formations. Moreover, soils prone to piping and tunneling, such as dispersive soils (Faulkner & *alii*, 2003; Valentin & *alii*, 2005; Shahrivar & *alii*, 2012), often show features of gully erosion.

Factors such as erodibility of substrates and soils, topography, neotectonic effects, land use or land cover changes, and climate change are considered as the main drivers of gullying. These factors are particularly common in large parts of Iran (Onwuemesi, 1990; Obiefuna & Adamu, 2012), where gully erosion occur especially in pediments, colluvial slopes and alluvial plains.

In the recent past the authors assessed various factors influencing gully erosion in the study area concentrating mainly on topographic settings, land use and vegetation

[1] *Faculty of Geographical Sciences and Planning, University of Isfahan, Isfahan, Iran.*
[2] *Department of Physical Geography, University of Tübingen, Rümelinstr. 19-23, 72070 Tübingen, Germany.*
[3] *Department of Science and Mathematical Engineering, Faculty of Petroleum and Mining Engineering, Suez University, Egypt.*
[4] *Department of Earth and Environmental Sciences, Pavia University, Italy.*
[*] *Corresponding author: REZA ZAKERINEJAD, r.zakerinejad@geo.ui.ac.ir*

(Zakerinejad & Maerker 2014, 2015) as well as morphotectonic characteristics (Zakerinejad & *alii*, 2016). However, an in-depth analysis of the role of the lithological composition of the substrates is still missing. For example, chemical aspects such as critical values of Sodium, Calcium and Magnesium have negative impacts on aggregate stability (Moghimi & *alii*, 2012). High values of the Sodium Absorption Ratio (SAR) are expressing the relative activity of sodium ions in the exchange reactions with the soil. Sodium when present in the soil in exchangeable form replaces calcium and magnesium adsorbed by the clays and causes dispersion of soil/substrate particles, and thus, facilitate gully erosion processes (Kemper & Koch, 1966; Servati & *alii*, 2008; Shahrivar & *alii*, 2012). Therefore, a comprehensive assessment of the lithologic composition influencing gully initiation is important to understand the spatial distribution of gully features. Therefore, in this study, we focus on the influence of the lithology and the resulting surface substrates on gully erosion in the Mazayjan (MZJ) catchment in southwestern Iran.

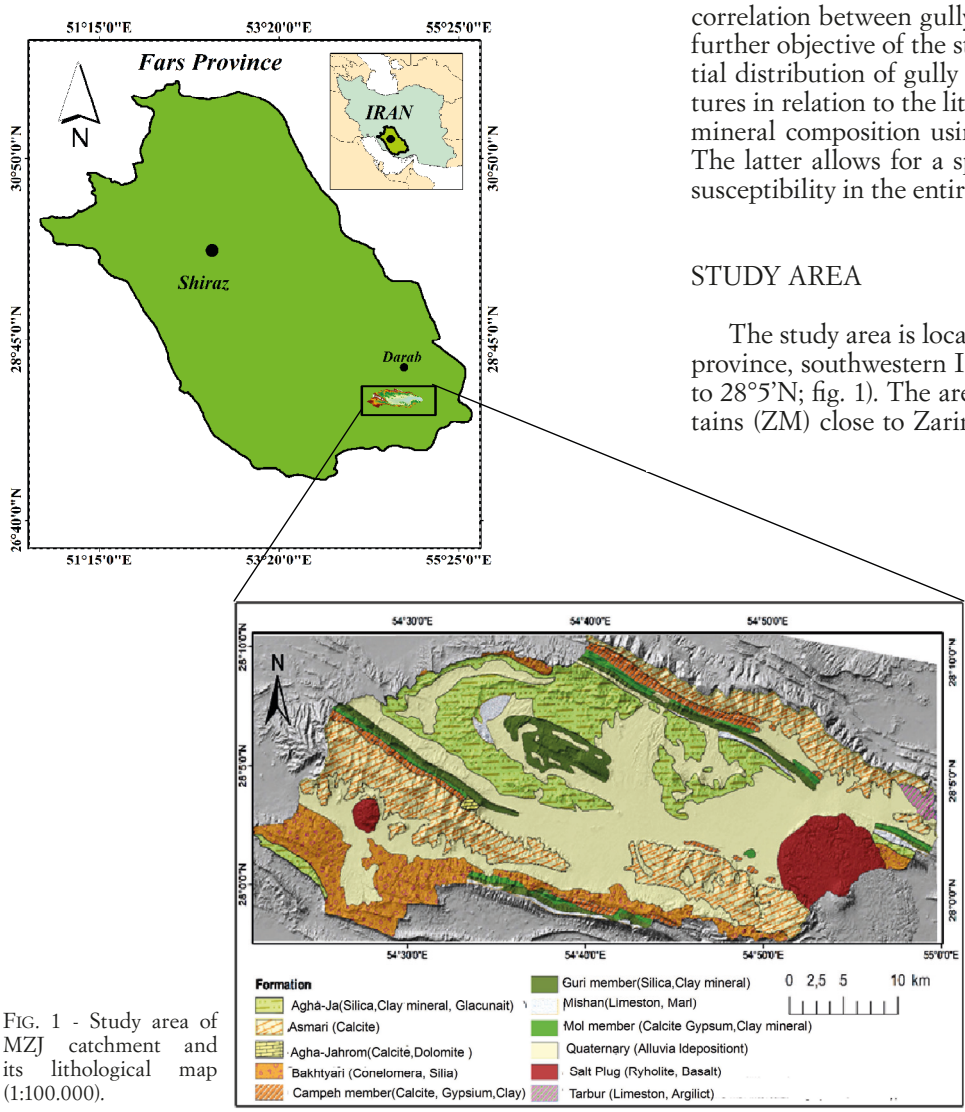

FIG. 1 - Study area of MZJ catchment and its lithological map (1:100.000).

Available geological and lithological maps were generated by the Iranian National Petroleum Organization (INPO) at the scale of 1:100,000 in 1954 and were mainly developed to identify different formations containing oil resources (Samani & *alii*, 2009). Generally, these maps were generated at large scales and are thus not very accurate in detail. However, no other more detailed geological map was produced since then. Therefore, we decided to utilize remote sensing data to obtain high resolution lithological information to assess gully erosion processes. In this study we use Advanced Space borne Thermal Emission and Reflection Radiometer (ASTER) spectral bands following the approaches presented by (Omran & *alii*, 2012) and (Matar & Bamousa, 2013). The study area is characterized by arid climate and sparse vegetation and therefore, well suited to examine the suitability of different ASTER band ratios to describe and map specific rock units and surface substrates (Omran & *alii*, 2012; Matar & Bamousa, 2013; Bachofer & *alii*, 2015).

The present study aims at proposing suitable ASTER band ratios appropriate to differentiate between different rock units and surface substrates in order to evaluate the correlation between gully location and mineral content. A further objective of the study is to assess the potential spatial distribution of gully erosion processes, forms and features in relation to the lithology characterized by a specific mineral composition using a statistical mechanics model. The latter allows for a spatial prediction of gully erosion susceptibility in the entire MZJ catchment.

STUDY AREA

The study area is located in the MZJ catchment of Fars province, southwestern Iran (54°34' to 54°44'E and 27°59' to 28°5'N; fig. 1). The area is located in the Zagros Mountains (ZM) close to Zarindasht city. The ZM belt extends for about 1500 km from the Taurus Mountains of southeastern Turkey, through southwestern Iran, ending near the Straits of Hormuz at the mouth of the Persian Gulf. This area is characterized by an arid climate with about 230 mm average annual precipitation and a mean annual temperature of 16.5°C. Field survey reveals that pediment and alluvial areas mapped as Quaternary deposits in the central part of the catchment, based on the 1:100,000 geological map, show significantly more gully systems. These gully systems in turn provide great amounts of sediments, which are transported into river systems or deposited in reservoirs and check dams within the catchment.

Era	Age	Formation	Legend	Symbol	Lithological Description	Minerals
Phanerozoic	Quaternary			Q	Composed of fragments to pebbles of purple graz siltstone. they are cemented mostly by gypsum. including marls, mudstone or shale.	Quartz, Kaolinite, Calcite, Halite
	Upper Pliocene to Pleistocene	Bakhtyari Fm.		Bk	Composed of boulder conglomerate with subordinate cross bedded sandstone and sandy siltstone. conglomerate are cemented with carbonate cement of the Caliche (calcerte)	Quartz, Calcite
	Upper Miocene to Pliocene	Agha Jari Fm.		Aj	Sequences of sandstone, mudstone to shales, sandy siltstone with marls and gypsum. Fine clastics contains light green Glauconite	Quartz, Glauconite, Kaolinite and Gypsum
	Lower to Middle Miocene	Mishan Fm.		Mn	Sequences of green marls, slightly gypsiferous inthe upper part as dominant part and limestonebeds at the lower part with silty sandstoneand sandy mudstone.	Quartz, Kaolinite, Gypsum and calcite
	Lower Miocene	Gachsaran Fm.		Champeh member (Cpm)	Composed of chalky gypsiferous limestone to dolostone with horizons of marls and nodular to crystalline gypsum .	Gypsum and calcite
				Mol member (Mlm)	Composed of reddish to multicoloured gypsiferous marls interbedded with gypsiferous limestone and gypsum .	Kaolinite, Gypsum, Calcite and hematite
	Oligocene to Lower Miocene	Asmari Fm.		As	Composed of mainly nummlilitic limestone .	calcite
Precambrian		Hamroz Fm.		Sp	- pale red to reddish brown siltstone . - interclation of dark dolostone, limestone conglomerates, ferrigenous and tuffogenic rocks contaning pyrite , siderite crystals and gypsum. - The center of the plugs composed of halite which covered other sedimentary rocks. Salts containing fragmentsto blocks of differents rock types .	Pyrite, gypsum, halite

FIG. 2 - Lithological and mineralogical description of the rock units in study area.

The study area is characterized by very sparse vegetation. The lowest elevation is 690 m and the highest peak of the ZM in the study area rises to 1969 m. Most of the gully features occur on the low sloping colluvial and pediment areas as well as on the plain covered by alluvial sediments (Zakerinejad & Maerker, 2014).

The geology of Hormuz is discussed by various authors such as Hull & Warman (1970); Gill & Ala (1972); Falcon (1974); Kashfi (1980); Edgell (1996); Bosak & *alii* (1998) and Bahroudi & Koyi (2004). Lithologically, the study area is subdivided into two main units (fig. 2). The first unit is Precambrian age and consists of salt plugs or glacial salts covering a total area of about109 km^2. The plugs are composed mostly of brownish gray to purplish gray siltstones, sometimes of pale red, purple or reddish brown color. The salt plugs are composed of weathered clay minerals, ferruginous minerals and some relicts from gypsum and halite at the distal part of the dome features. This unit has been subject to reductive environments which helped to form minerals like pyrite. Halite commonly occurs at the margins of plugs. Crystalline gypsum appears most often in brecciated form with fragments of shale, light-colored limestones and grayish brown siltstones. Dark gypsum with organic admixture and local intercalations of iron compounds are quite common.

The second unit consists of sedimentary Phanerozoic rocks of Cretaceous to Quaternary age with a total area of ca. 1300 km^2. Phanerozoic rocks are the main lithological formations exposed in the outcrops of the study area. The oldest rocks are the Asmari Formation (Oligocene to Lower Miocene) which cover about 200 km^2 of the study area. The Asmari Formation consists of dolomite, with dolostones and sandstones at the base, while the upper part is composed of a variety of limestone formations from nummulitic grainstones to fine-grained packstones. The Gachsaran Formation (Lower Miocene to Pliocene) is composed of the evaporitic Guri Member, the carbonate Champeh Member and the clastic-evaporitic Mol Member. The Mishan Formation (Lower to Middle Miocene) consists of bedded limestones, often chalky with an argillaceous admixture at the base, while the upper part is composed of mostly green marls, and in places is slightly gypsiferous with silty sandstone, sandy mudstone and sandstone interbeds.

The Agha-Jahri Formation (Upper Miocene to Pliocene) consists of alternating beds of sandstones, mudstones to shales and sandy siltstones. Finally, the youngest formation is the Bakhtyari Formation (Upper Pliocene to Pleistocene). This formation consists of pebble to boulder conglomerates with subordinate cross-bedded sandstones and sandy siltstones. Quaternary deposits have a large areal distribution of about 470 km^2. The Quaternary sediments are represented mostly by complex alluvial systems formed of coarse-grained, boulder conglomerates to gravels, which are often cross-bedded with minor sandy interbeds. A higher proportion of soft shales to marls, gypsum and anhydrite exist where the weathered materials derive from Miocene to Pliocene rocks. These sediments are enriched with gypsum, clay minerals (kaolinite) and salt minerals (halite).

MATERIALS AND METHODS

Materials

ASTER sensor is a joint collaboration between NASA and Japan's Ministry of Economy. The sensor carried by the TERRA satellite launched in December, 1999 (Fujisada, 1995; Matar & Bamousa, 2013) has 14 bands covering a vast spectral range: three bands in the Visible and one band in the Near Infrared (VNIR) with 15 m resolution; six bands in the Short Wave Infrared (SWIR) with 30 m resolution; and four bands in the Thermal Infrared (TIR) with 90 m resolution (Fujisada, 1995). The ASTER data of our study area were acquired on Feb. 28, 2006. Each scene covers an area of about 60 by 60 km (3600 km^2), which encompasses the MZJ catchment completely. In general, the SWIR bands were used for the discrimination of minerals or rock types (Yamaguchi & *alii*, 1998). First, the acquired data with compacted bands were separated and then processed by conducting radiometric and geometric corrections (Bachofer & *alii*, 2015). The scene used in this research is an ASTL1B of 14 bands dating from 2006. The image has been pre-georeferenced to UTM zone 40 with datum WGS 84 and ortho-rectified using a DEM. The proposed procedure to derive high resolution spatial information on the mineral composition of lithology and substrates using ASTER data mainly relies on the SWIR bands 4, 5, 6, 7, 8 and 9. The spectral ranges of the 30 m resolution SWIR bands are: 1.600-1.700 µm (band 4), 2.145-2.185 µm (band 5), 2.185-2.225 µm (band 6), 2.235-2.285 µm (band 7), 2.295-2.365 µm (band 8) and 2.36-2.43 µm (band 9).

Methodology

ROCK DIFFERENTIATION USING REMOTELY SENSED DATA - The rock differentiation may be carried out on the computer screen by human interpretation of the Aster images. This is a promising way in particular if the human operator is very experienced. To increase the degree of automation within the mapping process the tools of image classification can be employed. The analysis depends mainly on discriminating among the existing rocks types using their mineralogical composition, as illustrated in the processing workflow (fig. 3). The selected minerals are chosen based on the previous mineralogical studies of this area and confirmed by field visits. There were similarities in the mineral compositions of different rock formations, such as the Agha-Jahri sandstone formation and the Bakhtyari conglomerate formation, making it difficult to distinguish between them. Therefore, the analysis of the study area includes six sedimentary rock units, namely the salt plugs, Asmari, Gachsaran, Mischan, Agha-Jahri, Formations, and Quaternary sediments. Spectral indices derived from the ASTER VNIR and SWIR bands could help to deduce different mineral compositions and also emphasize the spectral differences of target objects (Bachofer & *alii*, 2015). Therefore, a band ratio stacking with the ratios of 4/9-4/6-9/8 is used for differentiation between the six sedimentary rock units.

Band rationing has been widely used for lithological mapping due to its proven ability to produce distinct grey tones of imaged materials in certain ratios. A band ratio is created by dividing the digital number (DN) of one band by the corresponding DN of another band for each pixel (Drury, 1987). The majority of fractional values are between zero and two or three. Thus, for visibility reasons the ratios are often rescaled to produce ratio images with higher contrast. Another well-known effect of rationing is the reduction of the impact of shadow in the ratio images.

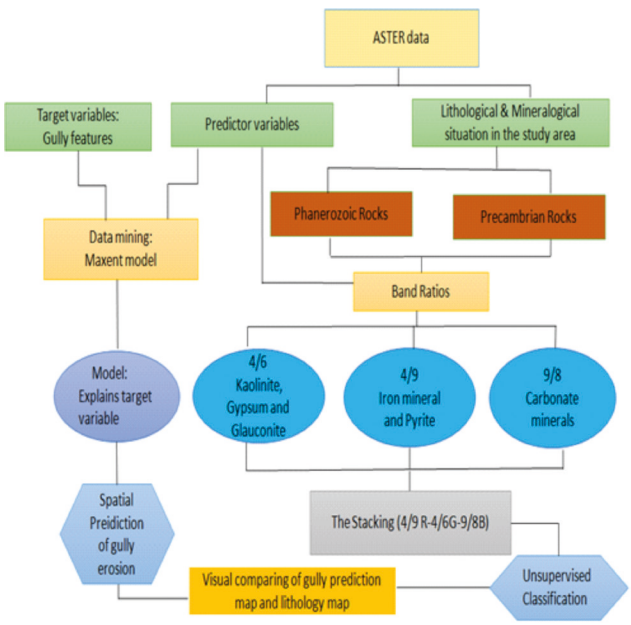

FIG. 3 - Flow chart showing the different steps of the mineral mapping approach.

Which band ratio is particularly suitable for enhancing a certain rock type or mineral depends on the dominance of the mineral in the reflected data. Spectral signatures give useful hints to decide about the bands used for rationing. Combinations of three band ratio images can be visualized as colour composites. Features or minerals show up in distinct colours in these stacked ratio images.

We decided to use calcite minerals to distinguish Phanerozoic units Oligocene-Lower Miocene carbonate rocks (Asmari and Gachsaran Formations). Consequently we used band ratio 9/8. Hematite and pyrite minerals discriminate Precambrian rocks (salt plug) so we applied band ratio 4/9. Moreover, we selected glauconite, gypsum and kaolinite to discriminate between Phaneroyic units Upper Miocene to Pliocene sandstone (Agha-Jahri Formation) and Middle Miocene rocks (Mischan Formation). Therefore band ratio 4/6 has been used.

The selected band ratios depended on their ability to identify the spatial signature of minerals characterizing the rock unit. The reflectance spectra of minerals were well known and catalogued, for example, in the USGS Digital Spectral Library (Clark & *alii*, 2007). The fact that rocks represent a complex mixture of materials limits the direct utilization of these spectra in remote sensing analysis. The use of the spectra is further reduced by the fairly broad bandwidth and the low number of spectral bands of ASTER.

To increase the degree of automation within the mapping process, we used image classification methods. In this study an Unsupervised Classification was conducted to show the different sedimentary classes in stacked layers. The majority of unsupervised classifications applied in this kind of studies are based on the Iterative Self-Organizing Data Analysis Technique (ISODATA) algorithm. The ISODATA algorithm was conducted using 7 classes and 10 maximum iterations and a convergence threshold of 0.95. The convergence thresholds of 0.95 stop the processing when 95% or more of the pixels remained in the same cluster between iterations. In the study we applied an ISODATA based unsupervised classification to get a first approximation of the spatial distribution of the lithological units and surface substrates.

STOCHASTIC MODELING OF GULLY EROSION - In this investigation the maximum entropy model (MEM) (Phillips & *alii*, 2006), is applied to predict the spatial distribution of gully susceptibilities and to reveal the most influencing triggering factors. MEM was successfully applied in environmental studies dealing with presence only data (Elith & *alii*, 2006; Howard & *alii*, 2012; Vorpahl & *alii*, 2012; Hosseini & *alii*, 2013; Zakerinejad & Maerker, 2014). MEM is one of the most commonly used methods for inferring species distributions and environmental tolerances from occurrence data and allows users to fit models of arbitrary complexity (Phillips & *alii*, 2006; Warren & Seifert, 2011). MEM provides a compressed description of data that is maximally noncommittal with respect to missing (unspecified) information (Jaynes, 1957; Wainwright & Jordan, 2008). In recent studies the method was used to predict the spatial distribution of soil erodibility, landslides and gullies using terrain parameters as independent variables

(e.g. Maerker & *alii*, 2014; Zakerinejad & Maerker, 2015; Mahamane, 2015). To assess the lithologic and surface substrate characteristics responsible for the spatial distribution of gully erosion features in this study we applied the Maxent version 3.3.3k (http://www.cs.princeton.edu/~schapire/maxent/). The model requires presence only data and a set of environmental variables which are continuously distributed in spatial extent (Zakerinejad & Maerker, 2014). In this case the probability distribution of gullies is estimated using the presence of gully features (dependent variable) and environmental predictor variables (independent variable) delineated from ASTER spectral information (single bands and ASTER band ratios).

We selected the six SWIR bands (4-9) and the SWIR band ratios (4/6; 4/9; 9/8) (fig. 3) as input features for the analysis. Finally, MEM also yields information on the impact of each predicator variable on the final model. MEM was trained and tested using a sample of 80% and 20%, respectively, of localities (cases) showing gully erosion phenomena. The gully features sample set was collected using the aerial photos (2003), Google earth (GE) and field survey at different locations of the study area in 2012.

Model Validation - The performance of the model has been evaluated using the receiver operator characteristic (ROC) curve for training and test data. Values close to 1 indicate that the model prediction is perfect, while values near or below 0.5 indicate a random prediction (Phillips & *alii*, 2006). In a ROC curve the true positive rate (sensitivity) is plotted over the false positive rate (1-specificity) for all possible cut-off points (Swets & *alii*, 2000). The area under curve (AUC) is a summary measure of the accuracy of a quantitative diagnostic test. According to (Hosmer & Lemeshow, 2000), AUC values exceeding 0.7/0.8/0.9 indicate acceptable/excellent/outstanding predictions. The contribution of the most important variables for the model is illustrated in the variable importance graph. Moreover, a jackknife graph which is a resampling technique especially useful for variance and bias estimation explores the variables with the greatest contribution to explain the distribution model and its importance when used alone (Phillips & *alii*, 2006; Elith & *alii*, 2011). Finally, we also show the most important variables plotted as a susceptibility or probability over the range of the variable parameters, identifying the relevant parts of the specific spectra contributing to the model.

RESULTS AND DISCUSSION

In the following section, we illustrate the results of the band ratio analysis to differentiate among the main lithological units using the mineral composition most appropriate for each rock unit. Then, we use the resultant band ratios describing the lithological units in an unsupervised classification to achieve a better spatial resolution of the geological units. Finally, we describe the results of the MEM approach utilized for the assessment of the relations between gully location and spectral band or band ratios.

Spectral band ratios and related lithology

Based on the geological map, the following band ratios were attributed to specific lithological units. The first band ratio 4/6 (fig. 4) best describes the Agha-Jahri Formation appearing in dark color due to its high concentration of glauconitic minerals (Bosak & *alii*, 1998), whereas the presence of gypsum and kaolinite minerals in the Mischan Formation produces a grey to light grey color (fig. 4). Gypsum deposits at the distal part of the salt plug zone are also discriminated well. Band ratio 4/9 especially characterizes Precambrian rocks because of their high contents in pyrite and iron minerals (hematite) (Bosak & *alii*, 1998). This rock unit appears darker than other rocks (fig. 5). Band ratio 9/8 identifies carbonate rocks with brighter color (white color) than other rock types. The rocks units (Asmari and Gachsaran Formations) are shown with white to light grey color in the scene, indicating their high carbonate content, whereas weathered minerals like gypsum and kaolinite

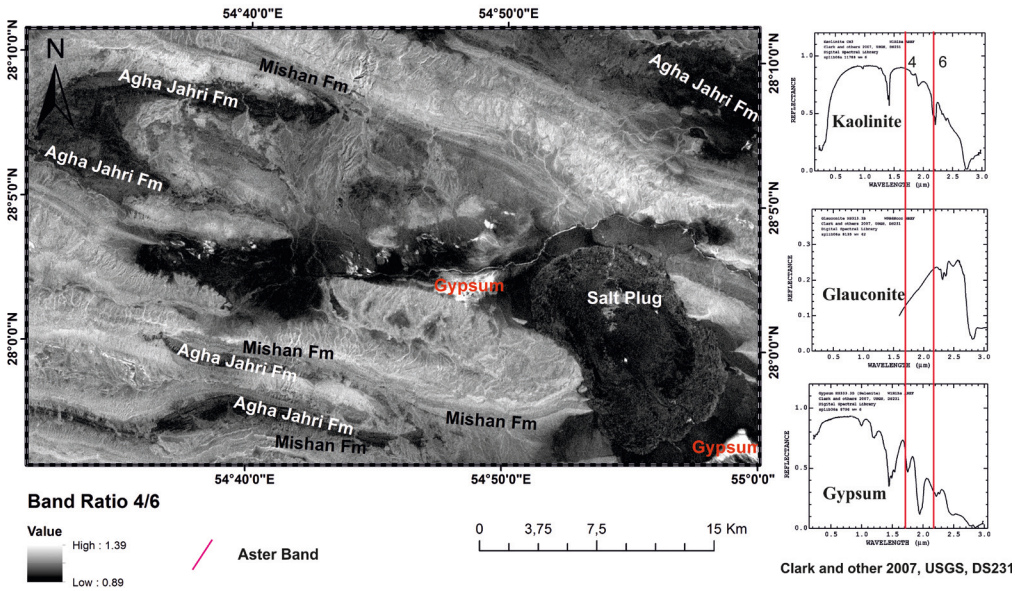

Fig. 4 - Ratio of band 4/6 of the MZJ catchment.

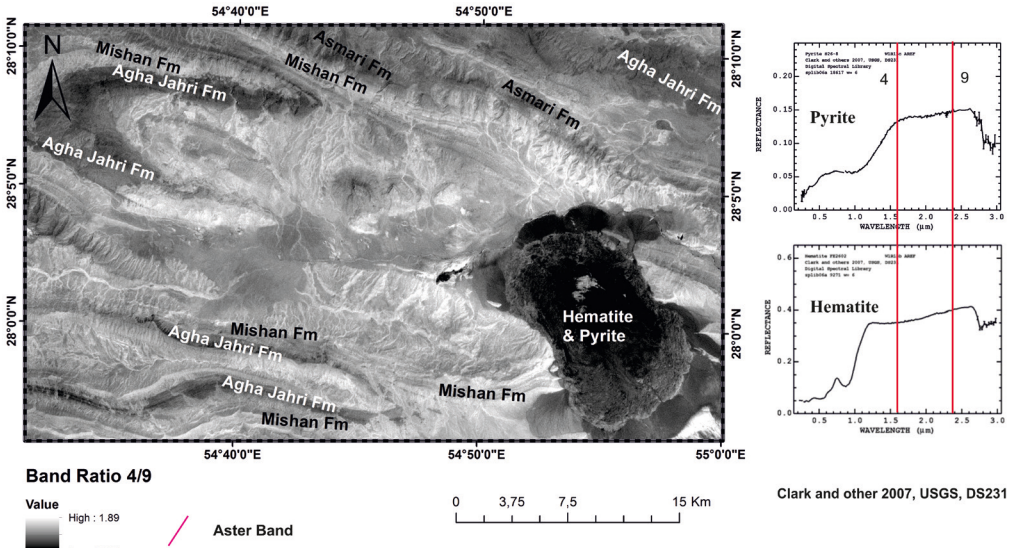

FIG. 5 - Ratio of band 4/9 of the MZJ catchment.

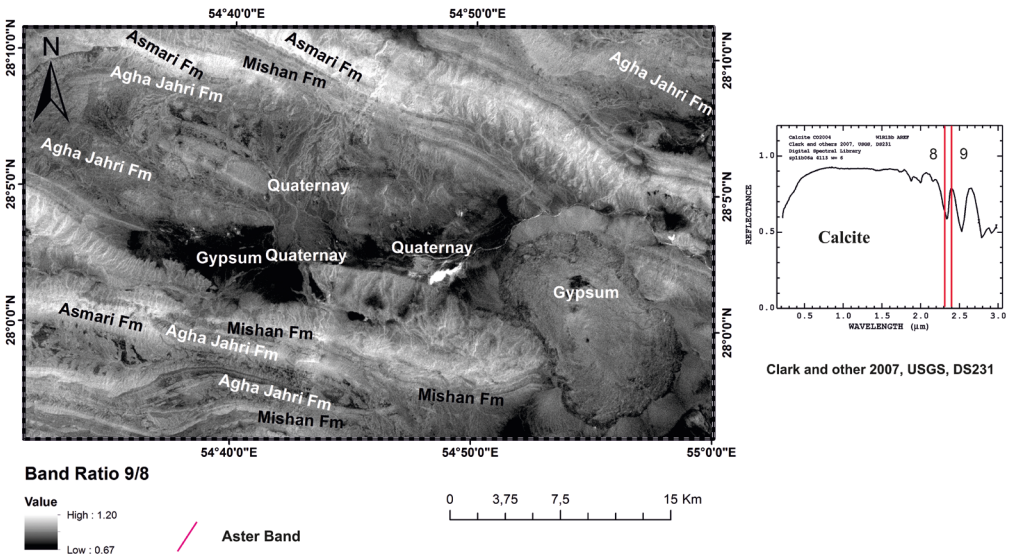

FIG. 6 - Ratio of band 9/8 of the MZJ catchment.

occur with dark grey to black color, especially in alluvial deposits (black color) (fig. 6).

In experiments with different band ratio stackings, we found that the color composite (4/9 R,4/6 G and 9/8 B) reveals subtle differences between the Asmari, Agha-Jahri and Mischan Formations on the one hand, and the salt plug and Quaternary rocks, on the other (fig. 7). Furthermore, the Asmari Formation appears in pale blue colors, the Agha-Jahri Formation in dark blue to purple, the Mischan Formation in dark yellow, the Gachsaran Formation in white, the Precambrian rock appears in blue to greenish blue, and the Quaternary deposits in brown to dark brown. The unsupervised classification is used as a first approximation of the lithological units using the stacking layer, as shown in fig. 8. The results of this classification cannot differentiate between Precambrian rocks and the Upper Miocene to Pliocene Agha-Jahri Formation in red. Additionally, the Mischan Formation is not well represented in this layer, with its pale blue and yellow color, since it is concentrated in very narrow strips occurring in the northeast and southwest of the study area adjacent to the Gachsaran Formation (Mol member). Moreover, the similarity of the mineral components of both formations makes it difficult to differentiate these units.

Nevertheless, this classification has distinguished the Asmari Formation in dark blue and the alluvial sediments (Quaternary deposits) into two classes (red and green). The reddish units are more related to the gypsum and kaolinite minerals which are represented by the main minerals components of the Agha-Jahri and Precambrian rocks. Instead the green color belongs to areas with low amounts of salt and gypsum deposition, especially in flat areas. Comparing field data from the gully locations and the results of this map we see that many gullies features are found in susceptible lithologies with high kaolinite, gypsum and salt concentrations. These components are mostly related to the Agha-Jahri formation, salt plugs and Precambrian rocks (fig. 8). However, a proper supervised classification was not

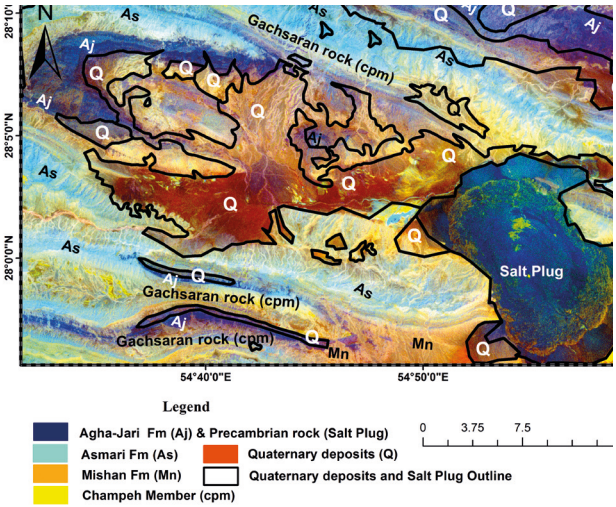

FIG. 7 - Stacking (4/9, 4/6, 9/8)-RGB of the MZJ catchment.

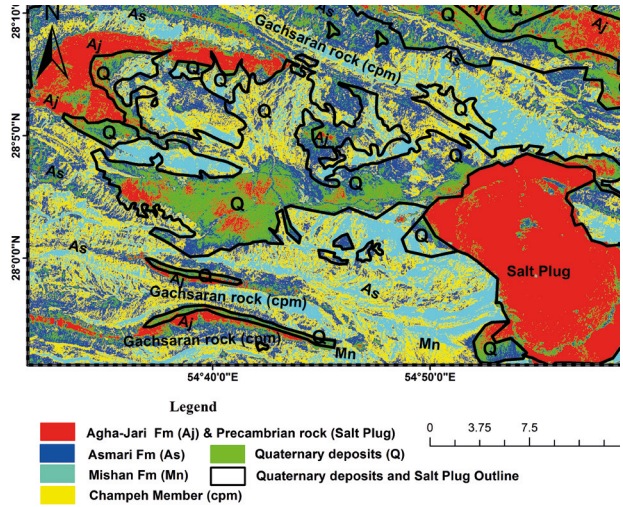

FIG. 8 - Unsupervised lithological classifications of the MZJ catchment.

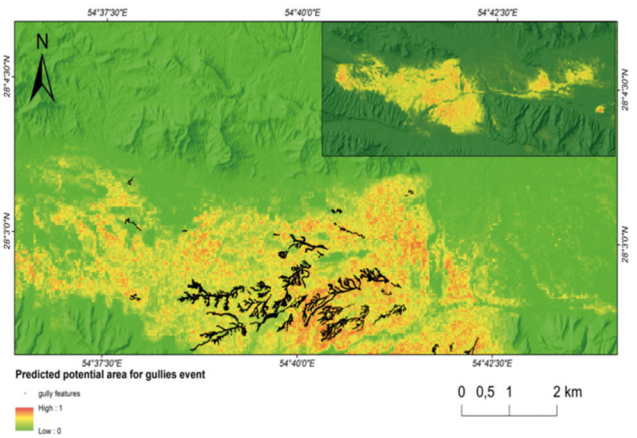

FIG. 9 - Predicted gully erosion susceptibilities in the MZJ basin.

possible due to a lack of field survey and the low scale of available geological maps.

Maxent modeling

In this research the Maxent model was applied to assess the relation between gully locations and ASTER spectral bands and/or band ratios representing specific lithologies. Moreover, the generated model was used to predict the susceptible areas for gully erosion in the MZJ catchment (fig. 9).To evaluate the performance of the applied model and its predictions, the data were divided randomly into training and test subsets, hence creating quasi-independent data for model testing (Fielding & Bell, 1997). Model results were evaluated using the ROC curves both for training and test data. According to fig. 9, the AUC values for training and test data are 0.97 and 0.96 respectively, indicating an outstanding model performance (Hosmer & Lemeshow, 2000). The most important variables indicating gully erosion are shown in tab. 1. The highest contribution

TABLE 1- The important variables.

SPECTRAL BANDS OR BAND RATIOS	PERCENT CONTRIBUTION	PERMUTATION IMPORTANCE
Band 9/8	54.6	46.4
Band 4/6	17.8	1.8
Band 7	14.4	2.4
Band 8	5.2	6.8
Band 4/9	4.6	14.6
Band 9	1.9	6.6
Band 4	1	3.8
Band 5	0.4	1.8
Band 6	0.2	15.8

to the model is band ratio 9/8, followed by band ratio 4/6 and band 7.

To get a proper insight into the main variables influencing the model results, we performed a jackknife test (fig. 11). The relevance of the band ratios and single bands for the modeled gully susceptibility can be identified in fig. 11. Based on to these results, band ratios 9/8 and 4/6 are the most effective in predicting susceptible gully areas. The important role of the band ratio 9/8 can be explained by the high content of siliceous material in alluvial deposits illustrated by dark grey to black color (fig. 5). Moreover, we analyzed partial dependency plots as univariate response curves by calculating non-parametric regressions from predicted values for single continuous predictor variables as a basis for interpreting the effect of predictors. Figure 12 shows the response curves for the important variables (band ratio 9/8, band ratio 4/6 and band 7). With regard to fig. 12a (X and Y axis shows band ratio and Probability of presence respectively), the band ratio 9/8 graph shows high probabilities below 0.80 and above 1.10. For the band ratio 4/6 values between 0.90 and 0.97 are related to high probabilities (fig. 12b), while band 7 is characterized by values

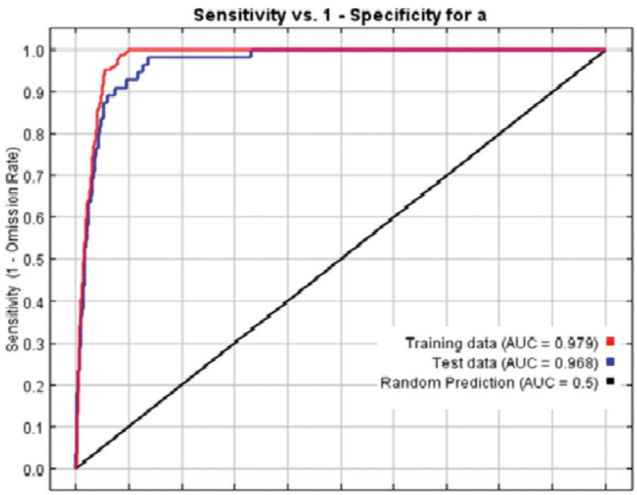

FIG. 10 - Area under ROC curve for validation of gully suitability model.

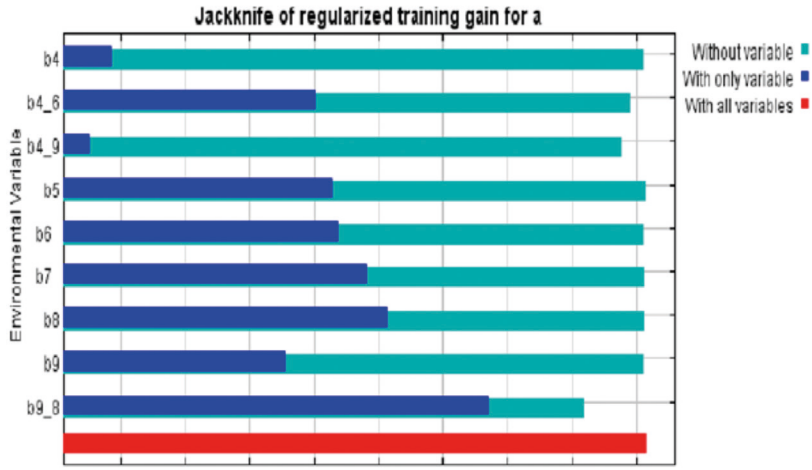

FIG. 11 - Jackknife test evaluating the relative importance of environmental predictors.

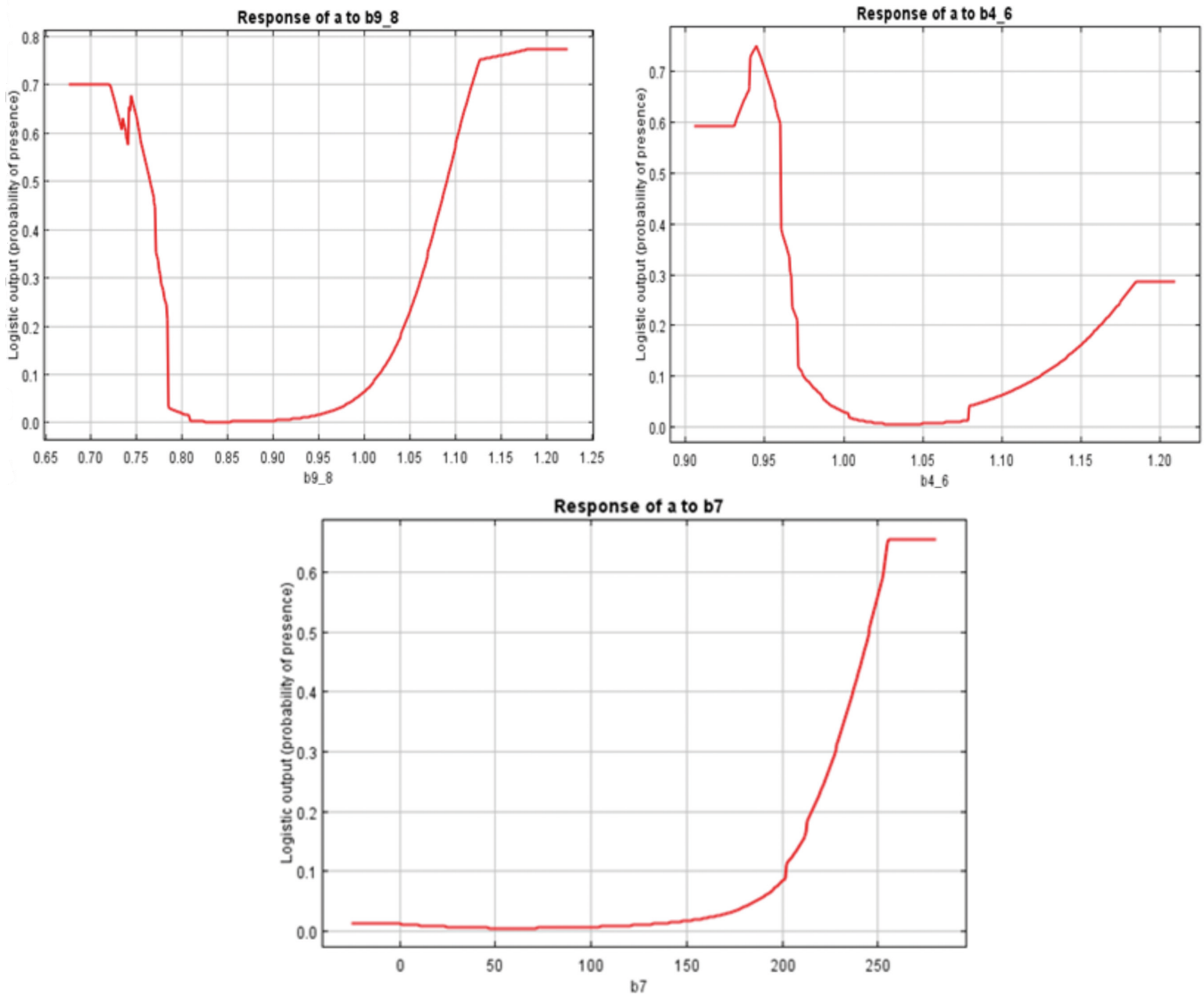

FIG. 12 - Responses curves of the most important predictors in the study area (band ratio 9/8, 4/6 and band7) - X and Y axis shows DN and Probability of presence respectively.

above 200 (Digital Number of the band) indicating higher probabilities (fig. 12c).

Prediction of gully erosion Susceptibilities

Figure 9 illustrates the spatial distribution of gully susceptibilities according to the lithology represented by different spectral bands and/or band ratios. Generally, it is shown that mountainous areas are less susceptible to gully erosion processes which in turn are mainly concentrated in the alluvial and colluvial parts of the catchment. Consequently, gullies occur especially in the plain areas in the west and east of the catchment (fig. 8). The locations of gullies highly correlate with the red signature especially in the plain/alluvial areas also revealed by GE image interpretation and a field survey conducted in March, 2012.

According to the predicted probabilities, the most susceptible areas for gullying are in the southwestern, western and eastern parts of the study area. These areas are characterized by Quaternary alluvial sediments where high amounts of salt, marl and gypsum are found and are, therefore, more susceptible to concentrated water erosion processes. Very high Electrical Conductivity (EC) and sodium adsorption ratio (SAR) values of soil samples measured in these areas indicate a high sodium content which amplifies gully erosion, as shown by various authors in the past (Faulkner & *alii*, 2003; Masoudi & Zakerinejad, 2010; Shahrivar & *alii*, 2012).

CONCLUSION

In this study we assessed the relation between lithology represented by different spectral bands and band ratios of the ASTER multispectral sensor, on the one hand, and gully locations mapped in the field and GE image interpretation, on the other. First, we identified the ASTER multispectral bands and band ratios that describe specific lithologies characterized by particular mineral compositions using the existing geological maps. With mineral differentiation analysis, different rock types like sedimentary rocks and Quaternary deposits in the ZM were distinguished.

Furthermore, we used the identified bands and band ratios with an unsupervised classification method in order to get a higher detailed geological differentiation of the area. Particularly the flat alluvial and colluvial parts are distinguished in a much greater detail and hence reveal a specific relation between gully sites and lithologic characteristics given by spectral band combinations. In the last step, we assessed these relations to reveal gully locations using a MEM approach developing a model that showed a strong influence of the band ratios 9/8 and 4/6, as well as band 7. This spectral information indicates high salt and sodium content, and hence high SAR and EC values, making the substrates particularly prone to gully erosion. The MEM model shows an outstanding performance for training and test data and is considered as a robust prediction tool. Finally, a map showing the spatial distribution of susceptible areas for gully erosion was derived, and it matches well with the gullies mapped by GE image interpretation and field survey.

The Maxent results showed that there was good correspondence between the locations of predicted gully areas and the results of mineral differentiation analysis using ASTER data. Gully features were mainly located in areas of alluvial deposition with loosely consolidated sediments and high kaolinite, gypsum and salt content.

In fact, the prevention of gully erosion is much easier and cheaper than trying to control it. With a predicted gully erosion map, it is much easier to identify prone areas and prevent against further soil loss. Therefore, prevention should be incorporated into all schemes of land management, in particular the identified prone areas in this part of the ZM of Iran. In this study we have shown that through the mineral differentiation analysis using ASTER data one of the main triggering factors for soil erosion and gullying in particular can be assessed with high spatial accuracy. However, all other factors like topography, climatic conditions and landuse land cover change should not be neglected and incorporated in further research to assess their degree of influence of the single driving factors and the sensitivity of the area towards these factors.

REFERENCES

Ahmadi H. (2007) - *Applied Geomorphology (water erosion)*. Tehran University, 688 pp. (in Persian).

Bachofer F., Quénéhervé G., Hochschild V. & Maerker M. (2015) - *Multisensoral Topsoil Mapping in the Semiarid Lake Manyara Region, Northern Tanzania*. Remote Sensing, 7, 9563-9586.

Bahroudi A. & Koyi H. A. (2004) - *Tectono-sedimentary framework of the Gachsaran Formation in the Zagros foreland basin.* Marine and Petroleum Geology, 21, 1295-1310.

Bosak P., Jaro J., Spudil J., Sulovsky P. & Václavek V. (1998) - *Salt Plugs in the Eastern Zagros, Iran: Results of Regional Geological Reconnaissance*. GeoLines, 7, 1-174.

Clark R.L., Swayze G.a., Wise R., Livo K. E., Hoefen T. & Kokaly R.F. (2007) - *USGS Digital Spectral Library*. U.S. Geological Survey.

Conoscenti C., Di Maggio C. & Rotigliano E. (2008) - *Soil erosion susceptibility assessment and validation using a geostatistical multivariate approach: a test in Southern Sicily*. Natural Hazards, 46, 287-305.

Drury S.A. (1987) - *Remote sensing of geologic structures in temperate agriculture terrains*. Geological Magazine, 123, 113-121.

Edgell H.S. (1996) - *Salt tectonism in the Persian Gulf Basin*. In G. I. Alsop, D. Blundell & I. Davison (Eds.), *Salt Tectonics*. Geological Society Special Publication, 100, 129-51.

Elith J., Graham C. H., Anderson R. P., Dudik M., Ferrier S., Guisan A. & Hijmans R.J. (2006) - *Novel methods improve prediction of species, distributions from occurrence data*. Ecography, 29, 129-151.

Falcon N.L. (1974) - *Southern Iran: Zagros Mountains*. In: Spencer A. (Ed.), Mesozoic-Cenozoic Orogenic Belts. Data for Orogenic Studies. Geological Society of London, Special Publication, 4, 199-211.

Faulkner H., Alexander R. & Wilson B.R. (2003) - *Changes to the dispersive characteristics of soils along an evolutionary slope sequence in the Vera badlands, southeast Spain: implications for site stabilisation*. Catena, 50, 243-254.

Fielding A.H. & Bell J.F. (1997) - *A review of methods for the assessment of prediction errors in conservation presence/absence models*. Environmental Conservation, 24, 38-49.

FRANKL A., POESEN J., DECKERS J., HAILE M. & NYSSEN J. (2012) - *Gully head retreat rates in the semi-arid highlands of Northern Ethiopia*. Geomorphology, 173, 185-195.

FUJISADA H. (1995)- *Design and performance of ASTER instrument*. Proceedings of the International Society for Optical Engineering, 2583, 16-25.

GHODOSI J. (2006) - *The effects of soil physico-chemical characteristics on gully erosion initiation.* 3rd Erosion and Sediment National Conference Soil Conservation and Watershed Management, 282-289.

GILL W.D. & ALA M.A. (1992) - *Sedimentology of Gachsaran Formation (Lower Fars Series), southwest Iran*. American Association of Petroleum Geologists Bulletin, 56, 1965-1974.

HOSMER D.W. & LEMESHOW S. (2000) - *Applied Logistic Regression 2nd ed*. Wiley, NewYork, 392 pp.

HOSSEINI S.Z., KAPPAS M., ZARECHAHOUKI M.A., GEROLD G., ERASMI S. & RAFIEIEMAM A. (2013) - *Modelling potential habitats for Artemisia sieberi and Artemisia aucheri in Poshtkouh area, central Iran using the maximum entropy model and geostatistics*. Ecological Informatics, 18, 61-68.

HOWARD A.M., BERNARDES S., NIBBELINK N., BIONDID L., PRESOTTO A., FRAGASZY D.M. & MADDEN M.A. (2012) - *Maximum entropy model of the Bearded Capuchin monkey habitat incorporating topography and spectral unmixing analysis*. ISPRS Annals of the Photogrammetry, Remote Sensing and Spatial Information Sciences, I-2.

HULL C.E. & WARMA H.R. (1970) - *Asmari Oil Fields of Iran, in M. T. Halbouty, ed.,Geology of Giant Petroleum Fields*. American Association Petroleum Geologists Memoir, 14, 428-437.

JAYNES E.T. (1957) - *Information theory and statistical mechanics*. Physics Review, 106, 620.

KASHFI M.S. (1980) - *Stratigraphy and Environmental Sedimentology of Lower Fars Group (Miocene), South-Southwest Iran*. American Association of Petroleum Geologists Bulletin, 64, 2095-2107.

KEMPER W. D. & KOCH E. J. (1966) - *Aggregate stability of soils from western USA and Canada*. USDA Technical Bulletin, 1355, US Government Printing Office, Washington, DC.

KHEIR R., WILSON J. & DENG Y. (2007) - *Use of terrain variables for mapping gully erosion susceptibility in Lebanon*. Earth Surface Process and Landforms, 32, 1770-1782.

MAERKER M., PAZ CASTRO C., PELACANI S. & SOTO BAUERLE M.V. (2008) - *Assessment of soil degradation susceptibility in the Chacabuco Province of Central Chile using a morphometry based response units approach.* Geografia Fisica e Dinamica Quaternaria, 31 (1), 47-53.

MAHAMANE M. (2015) - *Assessing soil erosion risk in the Tillabery landscape, Niger.* African Journal of Environmental Science and Technology, 9 (3), 176-191.

MASOUDI M. & ZAKERINEJAD R. (2010) - *Hazard assessment of desertification using MEDALUS model in Mazayjan plain, Fars province, Iran*. Ecology Environment and Conservation, 16 (3), 425-430.

MATAR S.S. & BAMOUSA A.O. (2013) - *Integration of the ASTER thermal infra-red bands imageries with geological map of Jabal Al Hasir area, Asir Terrane, the Arabian Shield*. Journal of Taibah University for Science, 7, 1-7.

MOGHIMI A.H, HAMDAN J., SHAMSHUDDIN J., SAMSURI A.W. & ABTAHI A. (2012) - *Mineralogy and aggregate stability of soils in the arid region of Southeastern Iran*. African Journal of Agricultural Research, 7 (11), 1639-1649.

OBIEFUNA G.I. & ADAMU J. (2012) - *Geological and Geotechnical Assessment of Selected Gully Sites in Wuro Bayare Area NE Nigeria.* Research Journal of Environmental and Earth Sciences, 4 (3), 282-302.

OMRAN A., HAHN M., HOCHSCHILD V., EL RAYES A. & GERIESH M. (2012) - *Lithological Mapping of Dahab Basin, South Sinai, Egypt using ASTER Data*. PFG. Schweizerbrat Science Publishers, 6, 711-726.

ONWUEMESI A.G. (1990) - *Hydrogeophysical and Geotechnical Investigation of the Ajali Sandstone in Nsukka and Environs with reference to groundwater resources and gully erosion problems*. Water Research: Journal of the Nigerian Association Hydrogeologists, 2 (1).

PHILLIPS S.J., ANDERSON R.P. & SCHAPIRE R.E. (2006) - *Maximum Entropy Modeling of species geographic distributions.* Ecological Modelling, 190, 231-259.

PICKUP G. (1991) - *Event frequency and landscape stability on the floodplain systems of arid Central Australia*. Quaternary Science Reviews, 10, 463-473.

PRINGLE H.J., WATSON I.W. & TINLEY K.L. (2006) - *Landscape improvement, or ongoing degradation - reconciling apparent contradictions from the arid rangelands of Western Australia*. Landscape Ecology, 21, 1267-1279.

SAMANI-NAZARI A., AHMADI H., JAFARI M. & BOGGS G. (2009) - *Geomorphic threshold conditions for gully erosion in Southwestern Iran (Boushehr-Samal watershed).* Earth Sciences, 35, 180-189.

SERVATI M.R., GHODDOSI J. & DADKHAH M. (2008) - *Factor effecting initiation and advancement of gully erosion in loesses*. Pejouhesh and Sazandegi, 20-33 (in Persian).

SHAHRIVAR A., TEHBCONSUNG C., JUSOP S., ABDUL RAHIM A. & SOUFI M. (2012) - *Roles of SAR and EC in Gully Erosion Development (A Case Study of Kohgiloyeva Boyerahmad Province, Iran).* Journal Research Agricultural Science, 8, 1-12.

SWETS J.A., DAWES R.M. & MONAHAN J. (2000) - *Better decisions through science*. Scientific American, 283, 82-87.

VALENTIN C., POESEN J. & YONG L. (2005) - *Gully erosion: impacts, factors and control*. Catena, 63, 132-153.

VORPAHL P., ELSENBEER H., MAERKER M. & SCHRÖDER B. (2012) - *How can statistical models help to determine driving factors of landslides?* Ecological Modelling, 239, 27-39.

WAINWRIGHT M.J. & JORDAN M.I. (2008) - *Graphical models, exponential families, and variational inference*. Foundation and Trends in Machine Learning, 1, 1-305.

WARREN D.L. & SEIFERT S.N. (2011) - *Ecological niche modeling in Maxent: the importance of model complexity and the performance of model selection criteria*. Ecological Applications, 21 (2), 335-342.

WASSON R.J., CAITCHEON G., MURRAY A.S., MCCULLOCH M. & QUADE J. (2000) - *Sourcing sediment using multiple tracers in the catchment of Lake Argyle, northwestern Australia*. Environmental Management, 29, 634-646.

YAMAGUCHI Y., KAHLE A.B., TSU H., KAWAKAMI T. & PNIEL M. (1998) - *Overview of advanced spaceborne thermal emission and reflection radiometer (ASTER).* IEEE Transaction on Geoscience and Remote Sensing, 36, 1062-1071.

ZAKERINEJAD R. & MAERKER M. (2014) - *Prediction of Gully erosion susceptibilities using detailed terrain analysis and maximum entropy modeling: a case study in the Mazayejan Plain, Southwest Iran*. Geografia Fisica e Dinamica Quaternaria, 37, 67-76.

ZAKERINEJAD R. & MAERKER M. (2015) - *An integrated assessment of soil erosion dynamics with special emphasis on gully erosion in the Mazayjan basin, Southwestern Iran*. Natural Hazards, 79, 25-50.

(Ms. received 04 March 2017; accepted 19 October 2018)